

Design Research on Contra-rotating Axial-flow Fan Silencers for Mining

Wang Xiang^{1,2}, Nie Yunhui^{1,2,3}

¹National Engineering & Technology Academy for Coal Mining, Huainan City, Anhui Province, 232001, China

²Ping'an Kaicheng Intelligent Security Equipment Co., Ltd., Huainan City, Anhui Province, 232001, China

³School of Safety Science and Engineering, Anhui University of Science and Technology, Huainan City, Anhui Province, 232001, China

Abstract: The contra-rotating axial-flow fan for mining is a local ventilator used in underground coal mining operations. However, the fan generates loud aerodynamic noises during operations, severely impacting the physical and mental health of operators as well as safe production. Based on the FBDNQ7.0/2*45 contra-rotating axial-flow fan for mining, this study employed model design, numerical simulations, and experimental validation to develop and design inlet and outlet silencers for the fan, so as to reduce fan noises to meet standard requirements, and carried out structural optimization on the silencers to reduce pressure losses and ensure the fan's operational efficiency.

Keywords: Axial-flow fan; Silencer; Numerical simulation; Noise control

1. Introduction

The contra-rotating axial-flow fan for mining in a dual-stage impeller design with counter rotation to generate high-pressure airflow, is widely applied in underground coal mines, typically tunneling workfaces and roadways in mining areas for localized dust removal, ventilation, and expelling methane gas and dust particles, to ensure operational safety. However, it may produce the noise of 90-120 dB during operations, which may even exceed 120 dB as the service life of the fan increases, and issues such as accumulated structural fatigue or component wear gradually emerge, far surpassing the noise limit of 85 dB prescribed in the *Coal Mine Safety Regulations*, and posing significant risks to both the physical and mental health of operators and production safety^[1].

A silencer is an environmental device that reduces fan operating noise by its structural design to suppress noise without impeding airflow passage. When designing a silencer of a contra-rotating axial-flow fan for mining, it must meet the specified noise reduction and airflow requirements at the fan inlet and outlet while maintaining the fan's efficiency^[2].

This paper investigated a contra-rotating axial-flow fan for mining, analyzed the initial noise levels of the fan, designed inlet and outlet silencers, optimized the internal structures through simulation calculations, and finally performed experimental validation by production trials.

2. Formation and Measurement of Fan Noise

2.1 Formation of fan noise

A fan typically generates three types of noise during operation: mechanical noise, electromagnetic noise, and aerodynamic noise^[3]. Mechanical noise is produced by physical vibrations, friction, or impacts during equipment operation, which can be effectively reduced by optimizing machining processes and performing timely maintenance and lubrication. Electromagnetic noise is generally caused by vibrations in certain mechanical components or in a volume of space by the alternating changes in the electromagnetic fields of motors, which, however, has a negligible impact in overall research and can be disregarded.

Aerodynamic noise is generated when fan blades rotate at high speeds, driving airflow to collide with the surrounding air. It is further categorized into rotational noise and vortex noise^[4]. Rotational

noise is generated by periodic impacts of blades against the surrounding air to create pressure pulsations. It is linearly related to the number of fan blades and rotational speed, and the calculation formula is shown.

$$f = \frac{nZi}{60}$$

In the Equation, f represents the frequency of rotational noise in Hz; n represents the rotational speed of the fan in r/min; Z represents the number of blades; i represents the higher-order frequency (1, 2, 3...).

Vortex noise arises from the viscous effects of air itself, and forms vortices on the blade's trailing edge, causing air turbulence, producing compression between air molecules and generating noise. The calculation formula is shown.

$$f = S_r \frac{V}{D} i$$

In the Equation, f represents the frequency of vortex noise in Hz; S_r represents the Strouhal Number; V represents the relative airflow velocity to the blade in m/s; D represents the object thickness in the direction of airflow incidence in m; i represents the ordinal number (1, 2, 3...).

In summary, the primary noise source during fan operation stems from aerodynamic noise. Due to high rotational speeds, the resulting rotational noise and vortex noise exhibited broad-frequency characteristics, with particularly pronounced mid-to-high frequencies.

2.2 Measurement of fan noise

The measurement subject is FBD No.7.0/2×45 contra-rotating axial-flow fan for mining manufactured by a certain enterprise as shown in Figure 1 below. Its main parameters are shown in Table 1.

Table 1 Parameters of FBDNo7.0/2×45 contra-rotating axial-flow fan for mining

Name	Parameters
Rated power	2×45(kW)
Maximum rotational speed	2960(r/min)
Airflow	400-700(m ³ /min)
Air pressure	1300-7400(Pa)
Number of front-stage blades	12
Number of rear-stage blades	10



Fig. 1 FBDNo7.0/2×45 contra-rotating axial-flow fan for mining

After determining that the surrounding environment free of background noise meets the experimental environment requirements, according to the standards GB/T 2888 “Noise Measurement Methods for Fans and Roots Blowers” and JB/T 8690 “Noise Limits for Industrial Ventilators”, the

measurement points shown in Fig. 2 were selected. After the calibration with the laser distance meter, the sound-level meter was turned on and set to A-weighted mode. Once the fan reached maximum power and operates stably, the data was measured at each point [5].

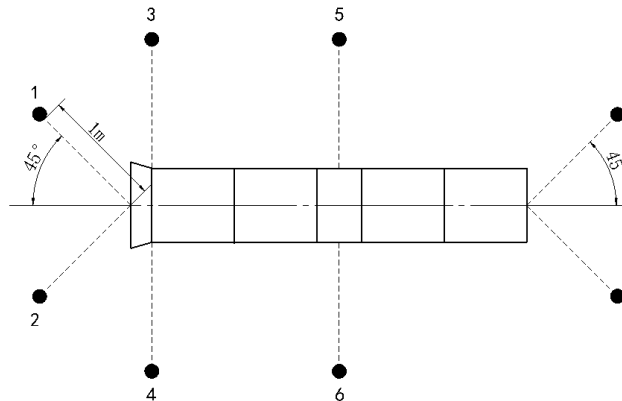


Fig. 2 Schematic diagram of measurement point distribution

The relevant data collected was exported from the test equipment to obtain the noise levels at each measurement point, as shown in the 1/3 octave band diagram in Fig. 3. It can be seen that the frequency characteristics at the inlet exhibited a broad-spectrum pattern, with a pronounced emphasis in the mid-to-high frequency range. The noise level in the frequency range of 500 Hz-2500 Hz was 78.1 dBA-88.5 dBA. The frequency characteristics at the outlet also exhibited a broad-spectrum pattern, with noise levels of 85.3 dBA-90.8 dBA in 500 Hz-800 Hz and 2000 Hz-4000 Hz.

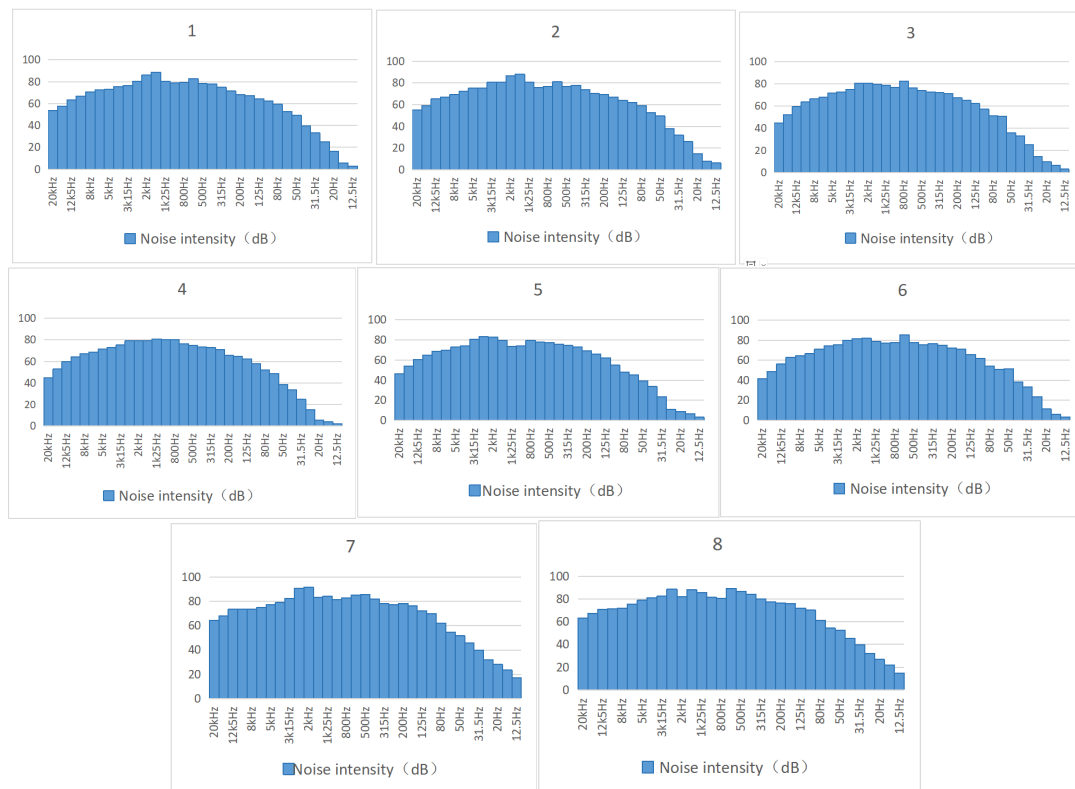


Fig. 3 1/3-octave band diagram of noise levels at measurement points without noise reduction measures

The sound pressure levels at measurement points are shown in Table 2. According to the *Coal Mine Safety Regulations* promulgated by the National Mine Safety Administration, the noise level in the working environment must not exceed 85 dBA. Thus, silencers must be designed for the fan inlet and outlet to enable the fan noise to meet the standard requirements.

Table 2 Sound pressure level at measurement points without noise reduction measures

Measurement point	Sound pressure level (dBA)	Measurement point	Sound pressure level (dBA)
1	92.7	5	89.3
2	93.1	6	90.0
3	89.9	7	96.2
4	89.8	8	96.6

3. Research on Design of Silencers

Silencers can be categorized into three types: resistive silencers, reactive silencers, and impedance composite silencers^[6]. Resistive silencers and impedance composite silencers have relatively complex internal structures that significantly impact fan airflow. In comparison, resistive silencers have simpler structures with lower pressure losses and deliver a superior effect of noise reduction at medium to high frequencies, which can meet the noise reduction requirements for the axial-flow fan for mining.^[7]

3.1 Design of the inlet silencer

To accommodate underground coal mine applications and operational efficiency of fans while reducing pressure losses, the structure of an inserted-plate silencer was adopted for the inlet silencer. The Equation for noise reduction of a resistive silencer is shown.

$$\Delta L = \Psi(\alpha_0) \frac{F}{S} \times L$$

In the Equation, ΔL represents the sound attenuation in dB; $\Psi(\alpha_0)$ represents the sound absorption coefficient (the sound absorption coefficient of glass wool at a density of 110 kg/m³ is 0.9 for all frequencies); F represents the cross-sectional perimeter of the silencer's airflow passage in m; S represents the cross-sectional area of the silencer's airflow passage in m²; L represents the effective length of the silencer, m.

According to the measured noise level at the fan inlet, a reduction of at least 9 dBA sound pressure level was required to meet the requirements. The primary structural dimensions of the inlet silencer were determined from the above Equation, specifically, the main body of 1300 mm in length with a frustum-shaped profile, an inlet outer diameter of 700 mm, an expansion diameter of 900 mm of the intermediate section, and three inserted plates spaced 180 mm apart of 50 mm thick each. The model is illustrated in Fig. 4.

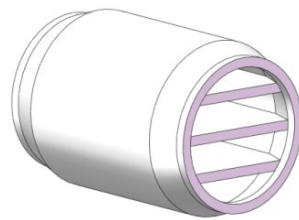


Fig. 4 The model of the inlet silencer

3.2 Design of the outlet silencer

Due to the high air volume and velocity at the fan outlet, the use of inlet silencer-like structure was unsuitable for safety considerations. To accommodate underground coal mine applications, the outlet silencer employed a resistive inserted-plate silencer elbow configuration. According to the measured noise level at the fan outlet, a reduction of at least 11 dBA sound pressure level was required. The primary structural dimensions of the outlet silencer were determined from the equation for sound attenuation, specifically, a length of 1050 mm, a width of 900 mm, and a height of 1000 mm. The base featured a semi-circular arc surface with a diameter of 900 mm. The arc-shaped inserted plates were employed, with inner diameters of 550 mm, 370 mm, and 160 mm respectively, with a thickness of 50 mm each and spaced 180 mm apart. The model is shown in Fig. 5.

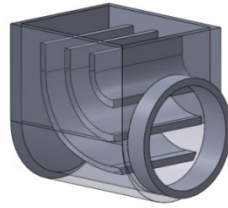


Fig. 5 The model of the outlet silencer

The housings and inserted plates of both silencers were uniformly filled with glass wool of 110 kg/m³ in density, and perforated plates were applied to the inner housings and inserted plates, providing effective suppression of low-frequency noise^[8].

3.3 Acoustic numerical simulation

Virtual Lab is a widely used simulation software in acoustic engineering and noise abatement, and is employed in this paper for acoustic numerical simulations.^[9]For computational accuracy and efficiency, the mesh was divided into two sections of 8mm-sized sound-absorbing material and air. These were defined as acoustic mesh properties with fluid material and properties set accordingly. The air sound velocity was set to 340 m/s, and the density to 1.225 kg/m³. The Delany-Bazley-Miki model was selected as the porous material model for the glass wool sound-absorbing material.^[10]perforated plates with inherent acoustic properties served as protective cover structures for silencers. In the Virtual.lab software, the structures of perforated plates could be represented by defining a transmission admittance matrix. A unit particle velocity of -1 m/s was assigned at the outlets of both silencers, with non-reflection boundary conditions defined at the outlets. The calculation frequency range was set to 100 Hz–2500 Hz. After calculations, the sound pressure response at the inlet and outlet were checked and the transmission loss calculations were performed. The transmission loss curve was exported. The sound field distribution nephograms extracted from the silencer at 800Hz are shown in Fig. 6.

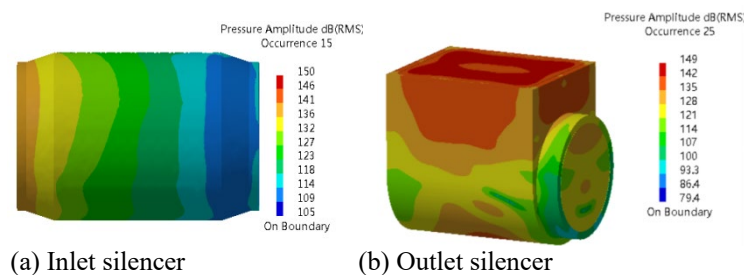


Fig. 6 Sound field distribution nephograms of two silencers at 800 Hz

The numerical simulation results are shown in Fig. 7. The transmission loss of the inlet silencer was represented by a straight line. At low and mid-frequencies, the transmission loss increased continuously with increasing frequency, reaching a peak of 38 dB at 1600 Hz. It began to decrease subsequently to 29 dB at 2000 Hz and 25 dB at 2500 Hz, before gradually stabilizing. The transmission loss of the outlet silencer increased continuously at low and mid-frequencies, reaching a peak of 27 dB at 1000 Hz. It remained relatively stable at 20-21 dB in the high-frequency range subsequently.

Although the peaks of insertion loss of the two silencers were different, both in general exhibited moderate attenuation at low frequencies and better attenuation at mid-to-high frequencies, consistent with the acoustic characteristics of resistive silencers.

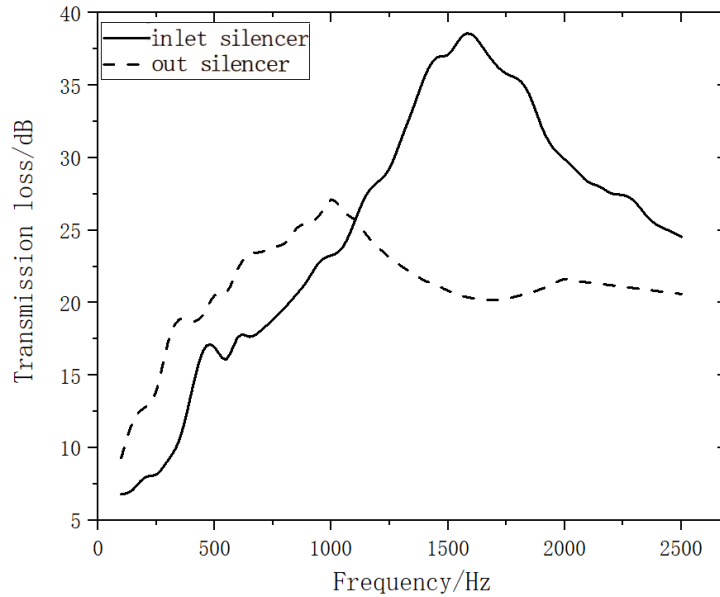
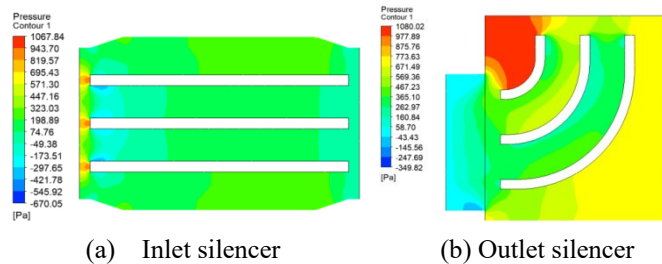


Fig. 7 Diagrams for transmission loss curves of two silencers

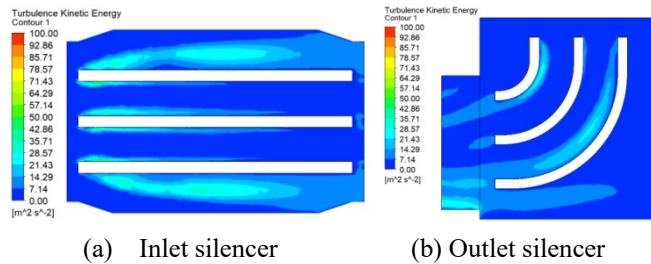
3.4 Internal flow field analysis of silencers

Fluent is a widely used simulation software in the field of fluid mechanics, and is applied in this paper for fluid numerical simulation. [1]The model was imported into the ICEM module for mesh generation and setting boundary conditions. The mass-flow-inlet was selected at the inlet, which was perpendicular to the inlet surface. The mass was calculated based on the axial flow of the axial-flow fan. The airflow operating condition of the axial-flow fan was set to 700 m³/min. The fluid was defined as incompressible and was solved by a pressure-based solver. The turbulence model equation employed the Realizable k-ε model, [12] which could effectively handle curved streamlines and transient flow. The pressure outlet at the silencer outlet was set to 0 Pa relative to atmospheric pressure. The inserted plates and walls of silencers were defined as wall with no slip. After completing the calculations, a symmetrical plane was selected to plot the nephograms for pressure and energy of turbulence of the two silencers, as shown in Figs. 8-9.



(a) Inlet silencer (b) Outlet silencer

Fig. 8 Nephograms for pressure of two silencers



(a) Inlet silencer (b) Outlet silencer

Fig. 9 Nephograms for energy of turbulence of two silencers

The nephograms for pressure and energy of turbulence were analyzed. The pressure was elevated at the front end of the inlet silencer's inlet inserted plate. The airflow directly impacted the inserted plate, causing increased localized pressure and inducing flow recirculation on both sides of the inserted plate,

resulting in significant airflow fluctuations. The outlet silencer was subjected to the earliest deflection of fluid flow at the shortest path through the inserted plate. The high-velocity air flow directly collided and mixed with the inserted plate and the low-velocity air flow at this point, resulting in elevated pressure. At the inlet face, the obstruction of air flow by the inserted plate caused a backflow on both sides of the plate. The greater the airflow fluctuations, the greater the energy losses. At the outlet, a sudden change in the cross section caused the air flow to impact the wall surface. And, vortex shedding occurred at the trailing edge of the inserted plate, causing mutual interference and the formation of complex wakes, as well as high turbulent kinetic energy.

In summary, the structure of the inserted plate was the primary factor impacting the internal flow field of the silencers and causing pressure losses. In order to stabilize the flow field of the silencers and reduce pressure losses, the structure of the inserted plate was optimized without compromising the silencer's acoustic performance by modifying the front and rear ends of the inserted plate into triangular shapes with a 30° apex angle to guide the airflow. An inlet silencer was selected for comparison, and numerical simulations were conducted again, with the results shown in Fig. 10.

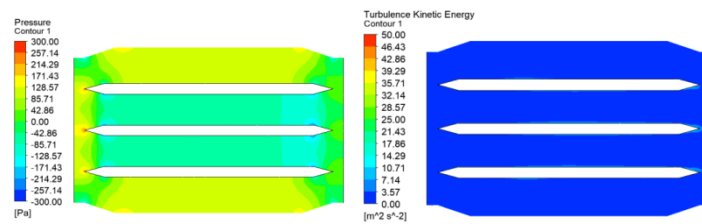


Fig. 10 Nephograms for pressure and energy of turbulence of the optimized inlet silencer

The optimized structure of inserted plate significantly improved the overall flow field of the silencers. The inserted plates exerted less resistance to the air flow, virtually eliminating backflow. The air flow passed through uniformly and stably, with reduced vortex shedding at the trailing edge of the inserted plate. The maximum turbulent kinetic energy decreased from 35 m²/s² to 7 m²/s². In addition, due to the reduced resistance of the inserted plate to air flow, the minor pressure gradient changes primarily occurred at the inlet and outlet cross-section variations of the silencers. The maximum pressure decreased from 1060 Pa to 300 Pa.

4. Experimental Validation

According to the analysis and conclusions of the paper, the inlet and outlet silencers shown in Figs. 11-12 were manufactured and mounted at the inlet and outlet of the FBDN_{07.0/2}×45 axial-flow fan for mining.



Fig. 11 Inlet silencer

Fig. 12 Outlet silencer

According to the experimental procedures, the fan was started until it reached stable operation, and then the relevant noise data was collected and the test results were exported as shown in Fig. 13. After mounting the inlet and outlet silencers, the sound pressure levels at measurement points decreased to some extent in the low-frequency range and reduced significantly in the mid-to-high-frequency range, respectively. The average reduction in sound pressure levels at measurement points in the fan inlet was

great at 800 Hz and 1000 Hz, reaching 21dB and 22.1dB, respectively. The average reduction in sound pressure levels at measurement points in the fan outlet at 1250 Hz and 1600 Hz was significant as 24.4dB and 31.5dB, respectively. The overall noise value trend was generally in alignment with the numerical simulation results. In actual measurements, sound waves at different positions interfered with each other, resulting in a slight reduction in the sound pressure level compared to the simulated values.

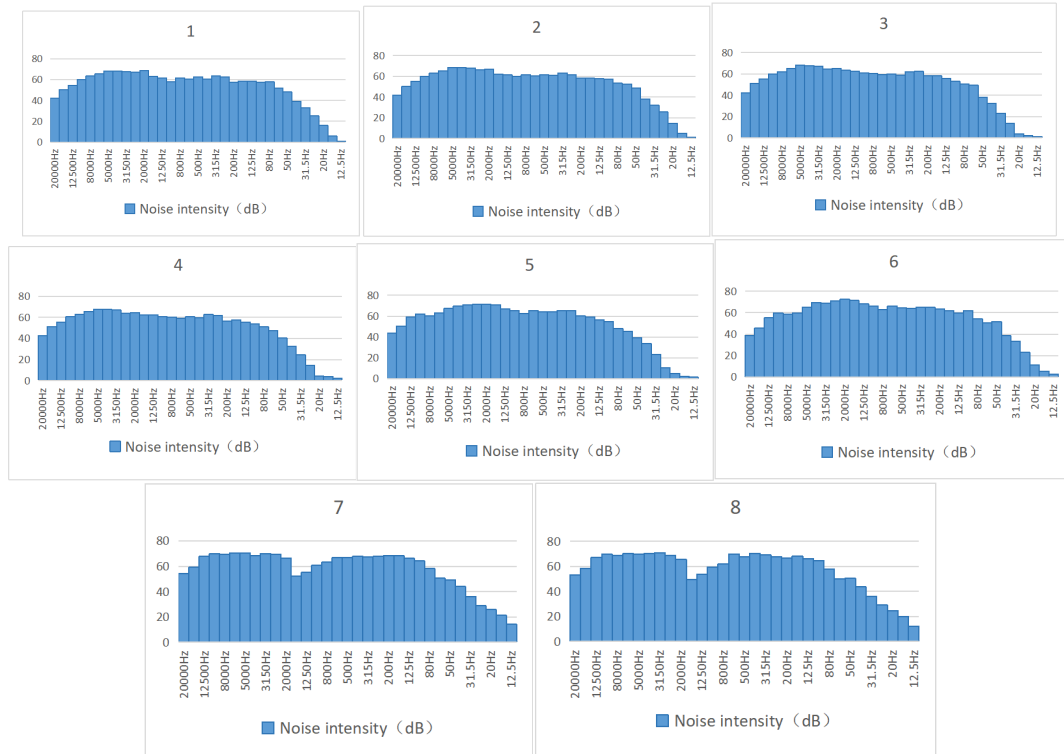


Fig. 13 Noise 1/3 octave band diagram at measurement points of the fan with silencers

As shown in Table 3, after mounting the silencers, the sound pressure levels at measurement points of the fan were below 85 dBA. Therefore, mounting the silencers at the fan inlet and outlet could meet national standards.

Table 3 Sound pressure levels at measurement points after mounting inlet and outlet silencers

Measurement point	Sound pressure level (dBA)	Insertion loss (dB)
1	77.3	15.4
2	77.1	16.0
3	76.3	13.6
4	76.3	13.5
5	79.9	9.4
6	80.1	9.9
7	81.1	15.1
8	81.0	15.6

5. Conclusions

For the issue of noise levels exceeding standard requirements during the operation of the contra-rotating axial-flow fan for mining, resistive silencers were designed for both the inlet and outlet of the fan in the paper, and acoustic and fluid simulations were conducted via numerical simulations.

The acoustic simulation results indicated that the inlet silencer exhibited significant noise reduction in the mid-to-high frequency range above 500 Hz, achieving a peaking transmission loss of 38 dB at 1600 Hz; the outlet silencer produced moderate noise reduction in the mid-to-high frequency range above 400 Hz, reaching a peaking transmission loss of 27 dB at 1000 Hz. The fluid simulation results indicated that the silencers' inserted plates were the primary cause of pressure losses. After optimizing

the structure of inserted plates of silencers, the maximum pressure of the inlet silencer decreased from 1060 Pa to 300 Pa, and the maximum turbulent kinetic energy reduced from 35 m²s⁻² to 7 m²s⁻², resulting in a significant improvement in the flow field. The experiments carried out on the inlet and outlet silencers designed for fans achieved a maximum insertion loss of 16 dB and a maximum noise level of 81 dBA. The overall results were consistent with the simulation results and fully met standard requirements.

References

- [1] H X Wu, et al. "[Hierarchical fuzzy comprehensive evaluation of prevention and control level of occupational hazards in coal mines]." *Chinese journal of industrial hygiene and occupational diseases* 42.1(2024):62-66.
- [2] Depies Chris R. "Discussion of design issues related to the application of industrial fan silencers." *INTER - NOISE and NOISE - CON Congress and Conference Proceedings 2001.1(2001):222-227.*
- [3] Mark Kelly, Emre Barlas, and Andrey Sogachev. "Statistical prediction of far-field wind-turbine noise, with probabilistic characterization of atmospheric stability." *Journal of Renewable and Sustainable Energy* 10.1(2018):013302.
- [4] Jiawei Shi, Jiye Zhang, and Tian Li. "Numerical Investigation on Aerodynamic Noise Source Identification and Far-Field Noise Characteristics of the High-Speed Train Bogie Region." *Acoustics Australia* 52.3(2024):1-17.
- [5] Wang Xiang. *Noise Control Technology and Research for Mine-used FBD Axial Flow Fans*. 2021. Anhui University of Science and Technology, MA thesis.
- [6] Ma, Dayou. *Handbook of Noise and Vibration Control Engineering*. Beijing: China Machine Press, 2002.
- [7] Li Da. *Research on Noise Analysis Prediction Model and Control Method for Cement Factory*. 2021. Anhui University of Science and Technology, MA thesis.
- [8] Liu, Canli. *Structure design and optimization of a multi-layer micro-perforated tube muffler based on the sound transfer matrix method*. Guangxi University of Science and Technology, 2018. Master's Thesis.
- [9] Zhang Xiaohui, et al. "Analysis of Fan Broadband Vortex Aerodynamic Noise and Noise Reduction". *Internal Combustion Engine & Powerplant* 40.04(2023):61-66.doi:10.19471/j.cnki.1673-6397.2023.04.009.
- [10] He Yuchen, et al. "Optimization Method for the Delany-Bazley Sound Absorption Model of Flat Polyester Fibers." *Technical Acoustics* 41. 02 (2022): 252-256. doi:10.16300/j.cnki.1000-3630.2022.02.016
- [11] Hong Xiaming. *Simulation of the airflow field of the grass collection component of the lawn mower based on Fluent and its experimental study*. 2025. Fujian Agriculture and Forestry University, MA thesis
- [12] Wei Zhiyong. *The Influence of Turbulence Models on the Numerical Simulation of Wind Turbine Aerodynamic Characteristics*. 2024. Dalian University of Technology, MA thesis